



Aalborg Universitet

AALBORG UNIVERSITY
DENMARK

Neural and muscular determinants of maximal rate of force development

Dideriksen, Jakob Lund; Del Vecchio, Alessandro; Farina, Dario

Published in:
Journal of Neurophysiology

DOI (link to publication from Publisher):
[10.1152/jn.00330.2019](https://doi.org/10.1152/jn.00330.2019)

Publication date:
2020

Document Version
Accepted author manuscript, peer reviewed version

[Link to publication from Aalborg University](#)

Citation for published version (APA):
Dideriksen, J. L., Del Vecchio, A., & Farina, D. (2020). Neural and muscular determinants of maximal rate of force development. *Journal of Neurophysiology*, 123(1), 149-157. <https://doi.org/10.1152/jn.00330.2019>

General rights

Copyright and moral rights for the publications made accessible in the public portal are retained by the authors and/or other copyright owners and it is a condition of accessing publications that users recognise and abide by the legal requirements associated with these rights.

- ? Users may download and print one copy of any publication from the public portal for the purpose of private study or research.
- ? You may not further distribute the material or use it for any profit-making activity or commercial gain
- ? You may freely distribute the URL identifying the publication in the public portal ?

Take down policy

If you believe that this document breaches copyright please contact us at vbn@aub.aau.dk providing details, and we will remove access to the work immediately and investigate your claim.

1 NEURAL AND MUSCULAR DETERMINANTS OF MAXIMAL RATE OF FORCE DEVELOPMENT

2

3 Jakob L. Dideriksen¹, Alessandro Del Vecchio², Dario Farina²

4 1: Department of Health Science and Technology, Aalborg University, Aalborg, Denmark.

5 2: Department of Bioengineering, Imperial College London, London, UK

6

7 RUNNING HEAD: Neural and muscular determinants of ballistic force

8

9 CORRESPONDING AUTHOR:

10 Jakob L. Dideriksen (jldi@hst.aau.dk)

11 Fredrik Bajers Vej 7D, 9220 Aalborg Ø, Denmark.

12

13 ABSTRACT

14 The ability to produce rapid forces requires quick motor unit recruitment, high motor unit discharge rates,
15 and fast motor unit force twitches. The relative importance of these parameters for maximum rate of force
16 development (RFD), however, is poorly understood. In this study, we systematically investigated these
17 relations using a computational model of motor unit pool activity and force. Across simulations, neural and
18 muscular properties were systematically varied in experimentally observed ranges. Motor units were
19 recruited over an interval starting from contraction onset (range: 22-233 ms). Upon recruitment, discharge
20 rates declined from an initial rate (range: 89-212 pps) with varying likelihood of doublet (inter-spike interval
21 of 3 ms; range: 0-50%). Finally, muscular adaptations were modeled by changing average twitch contraction
22 time (range: 42-78 ms). Spectral analysis showed that the effective neural drive to the simulated muscle had
23 smaller bandwidths than the average motor unit twitch indicating that the bandwidth of the motor output, and
24 thus the capacity for explosive force, was limited mainly by neural properties. The simulated RFD increased
25 by $1,050 \pm 281$ %MVC/s from the longest to the shortest recruitment interval. This effect was >4-fold higher
26 than the effect of increasing the initial discharge rate, >5-fold higher than the effect of increasing the chance
27 of doublets, and >6-fold higher than the effect of decreasing twitch contraction times. The simulated results
28 suggest that the physiological variation of the rate by which motor units are recruited during ballistic
29 contractions is the main determinant for the variability in RFD across individuals.

30

31 NEW & NOTEWORTHY

32 An important limit of human performance is the ability to generate explosive movements by means of rapid
33 development of muscle force. The physiological determinants of this ability, however, are poorly understood.
34 In this study we show using extensive simulations that the rate by which motor units are recruited is the main
35 limiting factor for maximum rate of force development.

36

37 KEYWORDS: Rate of force development, motor unit, computational model.

38

39 INTRODUCTION

40 The motor output is determined by the neural activation of the muscle (rate coding and recruitment of the
41 motor neuron pool) and the contractile properties of the motor units (the dynamics of the force twitches).
42 This implies that the characteristics of these parameters constrain the limits of muscle performance. One of
43 these performance limits is the ability to generate explosive force, usually characterized as the maximal rate
44 of force development (RFD). To achieve maximal RFD, high motor unit discharge rates, rapid recruitment of
45 the motor unit pool, and effective summation of motor unit twitches are required. For example, the initial
46 motor unit discharge rates during ballistic contractions are substantially higher than in slower contractions
47 (Desmedt and Godaux, 1977a; Del Vecchio et al., 2019b) and increase following prolonged training with
48 ballistic contraction (Van Cutsem et al., 1998). This increase may, at least in part, reflect a higher number of
49 so-called doublets (two discharges with very short inter-spike interval) (Van Cutsem et al., 1998; Christie
50 and Kamen, 2006; Mrówczyński et al., 2015). Furthermore, the force produced during electrically-induced
51 contractions when all motor units are recruited concurrently increases by a higher rate than during ballistic
52 voluntary contractions (de Ruyter et al., 2004; Folland et al., 2014) when motor units are recruited gradually
53 according to size (Desmedt and Godaux, 1977a, 1977b). Finally, muscles with high proportion of fast twitch
54 motor units exhibit the highest RFD (Desmedt and Godaux, 1978) and prolonged training with ballistic
55 contractions involves shortening of the average twitch contraction time (Gruber et al., 2007). Although the
56 neural and contractile factors influencing rate of force development have been discussed previously
57 (Duchateau and Baudry, 2014; Folland et al., 2014; Del Vecchio et al., 2019b), their relative importance is
58 not known.

59 Recently, we showed that the variance in human RFD is associated to the maximal motor unit discharge rate
60 and to the latency from the recruitment of the first to the last motor unit (recruitment interval) (Del Vecchio
61 et al., 2019b). However, it was not possible to evaluate the relative importance of the neural and contractile
62 parameters on RFD due to the unknown variance in motor unit twitches among subjects. For this reason, here
63 we aimed to investigate the neural and muscular determinants of maximal RFD using a realistic
64 computational model of a ballistic isometric contraction to a stable near-maximal contraction level. This
65 model allowed systematic variations of the motor unit discharge rate (including the chance for occurrence of
66 doublets), the rate by which motor units were recruited (determining the time interval until full recruitment),
67 and the motor unit twitch contraction times. The ranges of values assigned to these parameters were derived
68 from our recent experimental study (Del Vecchio et al., 2019b), as well as previously published experimental
69 findings.

70 The simulation results were analyzed in two complementary ways. First, the neural and muscular properties
71 were analyzed in the frequency-domain and their bandwidths were compared. This analysis was based on the
72 notion that motor unit force can be described as the convolution between the motor neuron spike train and

73 the motor unit twitch force. Thus, the power spectrum of the force generated by each motor unit is the
74 product of the power spectrum of the spike train and the square magnitude of the Fourier transform of the
75 twitch force. Similarly, the power spectrum of the total force can be approximated as the product of the
76 power spectrum of the neural drive to the muscle (sum of all motor unit spike trains) and the square module
77 of the average motor unit twitch force (average force twitch response over all active motor units). In this
78 way, the average motor unit twitch can be regarded as a filter for the neural drive and the characteristics of
79 the motor output is determined by this filtered neural drive. The power of the filtered neural drive determines
80 the magnitude of the force, while its bandwidth reflects the speed of the force: The larger the bandwidth, the
81 greater the ability to produce rapid forces. If the neural drive contains high frequencies, but these are filtered
82 out by the twitch, the twitch would be the limiting factor for the output. Thereby the muscular properties
83 would be the main determinant for RFD, and vice versa. In the second part of the analysis, the RFD was
84 calculated for all combinations of values assigned to the main model parameters. This enabled direct
85 comparison of the degree to which each parameter affected RFD. The outcome of both analyses showed that
86 the main determinant of maximal RFD was the rate by which motor units were recruited.

87

88 METHODS

89 *Experimental data*

90 The experimental data was adopted from a previous study (Del Vecchio et al., 2019b). In that study, 20 men
91 (age: 24.9 ± 3 yr, weight: 75.4 ± 8.6 kg, height: 180 ± 10 cm) performed isometric ankle-dorsiflexion
92 explosive force contractions. Participants were instructed to contract as fast and as forceful as possible and
93 then hold force at levels above 75% of the maximum force. The force signals were recorded concurrently
94 with high-density surface electromyography, which was decomposed into individual motor unit
95 contributions. On average, 12.1 ± 5.7 motor units were decomposed per contraction. Across all subjects, the
96 motor units initially exhibited a few discharges with very short inter-spike interval (as low as 4.7 ms) after
97 which the discharge rate declined steadily over a period of 200-300 ms. This behavior is compatible with
98 discharge patterns observed in previous studies (Granit et al., 1963; Desmedt and Godaux, 1977a; Van
99 Cutsem et al., 1998). After this period, a steady discharge rate was observed (mean: 37 ± 8 pulses per
100 second; pps). Figure 1 summarizes the relevant data from the experiment. Across the 20 subjects, the average
101 initial discharge rate and ranged between 89 and 212 pulses per second (pps; mean: 132 ± 31 pps; Fig. 1A).
102 Within each subject, the initial discharge rate did not depend on the recruitment threshold. The recruitment
103 interval ranged between 22 to 117 ms (mean: 60 ± 28 ms; Fig. 1B). The RFD was expressed in units % of
104 MVC/s. RFD ranged from 350 to 654 %MVC/s (mean: 442 ± 85 %MVC/s) (Fig. 1C).

105 *Computational model*

106 Motor unit spike trains were based on a predefined function describing the discharge rate. This function
107 contained a linear decrease from the assigned initial discharge rate (see *Simulations*) to 37 pps over a period
108 of 250 ms (Del Vecchio et al., 2019b). After this period, the discharge rate remained constant. This template
109 was applied to all motor units of the pool, but noise was added individually for each motor unit to ensure a
110 coefficient of variation for the inter-spike interval of approximately 10% (Matthews, 1996; Moritz et al.,
111 2005). In addition, the model included simulation of doublets by additional discharges 3 ms after a
112 predefined percentage (see *Simulations*) of randomly selected simulated discharges.

113 The smallest motor unit was recruited at the onset of the contraction and the recruitment time of the other
114 motor units was exponentially distributed throughout the assigned recruitment interval (see *Simulations*). In
115 this way, most motor units were recruited in the first period of the recruitment interval, whereas the largest
116 motor units were recruited at the end, as previously observed (Desmedt and Godaux, 1977a).

117 The isometric force was simulated from the discharge patterns based on a modified version of the model
118 proposed by Fuglevand et al. (Fuglevand et al., 1993). Since this model reflected the first dorsal interosseous,
119 the model was adapted to reflect the tibialis anterior muscle. This involved setting the number of motor units
120 to 188 (Xiong et al., 2008). Furthermore, the proportion of type II muscle fibers in the first dorsal
121 interosseous is approximately 50% (Fuglevand et al., 1993; Enoka and Fuglevand, 2001) while it is 30% in
122 the tibialis anterior (Henriksson-Larsén et al., 1983). By replacing Eq. 15 in (Fuglevand et al., 1993) by a
123 linear distribution from 90 to 30 ms, the proportion of muscle fibers with contraction times <35 ms was
124 reduced from 50% to 30%. The smallest motor unit was assigned the highest contraction time. As in the
125 original version of the model, there was a 100-fold range of twitch amplitudes across the motor unit pool,
126 since this range is compatible with experimental data for the tibialis anterior (Van Cutsem et al., 1998).

127 Next, a more detailed model for the non-linear gain of the twitch amplitudes was implemented. During trains
128 of action potentials, the amplitude of the motor unit twitch increases with respect to the first twitch, with a
129 factor that depends on the interval between the action potentials (Burke et al., 1976). In the original version
130 of the model, this gain was modeled based on experimental observations of the twitch after more than three
131 action potentials. This gain, however, depends on the inter-spike interval in a different way for the second
132 and third action potential (Burke et al., 1976). Whereas this difference has a small influence on simulations
133 of sustained contractions, which was the primary focus of the original model (Fuglevand et al., 1993), it may
134 have a substantial impact on simulations of ballistic contractions involving a small number of discharged
135 action potentials. Consequently, the twitch gain (G) was modeled as a function of the inter-spike interval
136 (ISI) normalized to the twitch contraction time (CT) as follows:

$$G = 0.84 \frac{ISI^3}{CT} - 3.08 \frac{ISI^2}{CT} + 1.16 \frac{ISI}{CT} + 4.33, \text{ for } AP\# = 2$$

$$G = 1.14 \frac{ISI^3}{CT} - 5.84 \frac{ISI^2}{CT} + 7.23 \frac{ISI}{CT} + 1.19, \text{ for } AP\# = 3$$

$$G = 1.29 \frac{ISI^3}{CT} - 6.91 \frac{ISI^2}{CT} + 9.82 \frac{ISI}{CT} - 0.89, \text{ for } AP\# \geq 4$$

137 Where AP# denotes the action potential number. The gain was limited to values >1 and was set to 1 for
 138 normalized inter-spike intervals >2.3. Figure 2 illustrates these relations along with the experimentally
 139 observed values (Burke et al., 1976). R² between the simulated parameters and the experimental values was
 140 0.97, 0.92, and 0.97 for the second, third, and fourth action potential, respectively.

141 *Simulations*

142 Across the simulations, the discharge rate was varied either by changing the initial discharge rate or by
 143 increasing the chance of doublets. In the first set of simulations, three different values were assigned to the
 144 initial discharge rate (minimum, median and maximum experimentally observed values: 89, 132, 212 pps;
 145 Fig. 1A). In each simulation, one of these rates were assigned uniformly to all motor units. In these
 146 simulations the chance of doublets was set to 0%. In another set of simulations, the chance of doublets was
 147 set to 0%, 25%, or 50%. Again, in each simulation, this rate applied to all motor units. At 50%, on average
 148 every 2nd discharge assigned a doublet (an additional discharge after 3 ms), which is equivalent to the rate of
 149 inter-spike intervals <5 ms observed for the first few discharges after 12 weeks of explosive training (Van
 150 Cutsem et al., 1998). Although it is not clear if this chance of doublets occurring remains stable throughout
 151 the rest of the explosive contraction, this rate was imposed on the entire simulation since doublets have also
 152 been observed in sub-maximal steady contractions (Kudina and Andreeva, 2010). In simulations varying the
 153 chance of doublets, the initial discharge rate (discounting doublets) was set to 132 pps.

154 Five values were assigned to the recruitment interval distributed in 8 evenly spaced intervals between 22 ms
 155 (lowest experimentally observed value; Fig. 1B) and 233 ms. The upper bound of this range (233 ms) was set
 156 to twice the highest value experimentally observed by EMG decomposition (Del Vecchio et al., 2019b). This
 157 choice was motivated by the fact that EMG decomposition provides a relatively small sample of the active
 158 motor units and therefore it is unlikely that the first and/or the last recruited motor units are identified in
 159 EMG decomposition studies. This leads to an underestimate of the recruitment interval. Accordingly, pilot
 160 simulations showed that the slowest experimentally observed RFD (<400 %MVC/s; Fig. 1C) could only be
 161 obtained in simulations with recruitment intervals longer than the maximal value previously observed in the
 162 experiments. Furthermore, three gains were applied to the motor unit twitch contraction times (CT-gain): 0.7
 163 (fast motor units; average contraction time: 42 ms), 1 (normal motor units representing the expected values
 164 for tibialis anterior; average contraction time: 60 ms), and 1.3 (slow motor units; average contraction time:
 165 78 ms). This range of gains was selected to reflect the largest adaptations in contraction time observed

166 following different types of resistance training (Schmidtbleicher and Haralambie, 1981; Pääsuke et al., 1999;
167 Gruber et al., 2007; Jenkins et al., 2016). To summarize, the ranges described above for the model
168 parameters represent the entire realistic range of values for the three parameters.

169 The ballistic force was simulated using every combination of these parameters (total of 150 different
170 combinations) and each of these simulations was repeated six times. The duration of each simulation was
171 500 ms, since a peak in the rate of force development was achieved earlier than 500 ms into the contraction
172 across all settings. For each simulated ballistic force, the RFD was calculated in the same way as for the
173 experimental data (unit: %MVC/s). The MVC was estimated individually for each CT-gain as the average
174 force produced during a 3-s simulation (excluding the first second) with the discharge rate for all motor units
175 set to 60 pps (Enoka and Fuglevand, 2001).

176 The cut-off frequencies of the neural drive (sum of spike trains from all motor units) and the average twitch
177 (weighted by twitch amplitudes) were estimated from their power spectra as the frequency at which the
178 power had decreased by 50% with respect to the maximal power equivalent to decline of 3 dB.

179

180 RESULTS

181 Figure 3 shows examples of the neural drive (smoothed cumulative spike train) and the average motor unit
182 twitch force in the time and frequency domain from simulations with different settings. The power spectra
183 were derived from the interval that reflected the RFD (the period from 0% of MVC to the maximum RFD).
184 In the simulation with relatively long recruitment interval (172 ms) and median initial discharge rate (132
185 pps) (black unbroken line in Fig. 3A), the magnitude of the neural drive (density of motor unit action
186 potentials) peaked approximately 88 ms after the onset of the contraction (time=0). The decrease in neural
187 drive after the peak reflected the gradual decrease in discharge rate to approximately 37 pps. Increasing the
188 initial discharge rate for the motor units (212 pps; black dashed line) implied a higher peak magnitude of the
189 neural drive, but no substantial difference in time to peak (83 ms after contraction onset). Consequently, the
190 cut-off frequencies of the power spectra of the neural drives in these conditions were similar (2.1 Hz for both
191 low and high initial discharge rate, respectively; black unbroken and dashed lines, Fig. 3B). This implies that
192 although an increase in the initial discharge rate involved increased power of low-frequency neural drive
193 components, it does not lead to large improvements in the ability to produce rapid force. Introducing a 50%
194 chance of doublets (grey unbroken line, Fig. 3A and 3B) had almost the same effect as increasing the
195 discharge rate to 212 pps in the time and frequency domain. Since a 50% chance of doublets is equivalent to
196 an effective discharge rate 198 pps, this indicates that the neural drive is determined by the net number of
197 discharges and not their specific timing. In other words, the same changes in the neural drive can be obtained
198 by increasing the average discharge rate or by increasing the chance of doublets. Contrary to the impact of

199 rate coding on the power spectrum of the neural drive, the cut-off frequency of the neural drive increased
200 substantially (4.3 Hz) when the recruitment interval was reduced (22 ms; grey dashed lines in Fig. 3A and
201 3B). This implied an increase in the ability to support rapid force generation. Therefore, changes in rate
202 coding affected the bandwidth of the neural drive to a smaller extent than the rate of recruitment.

203 The duration of the compound motor unit twitch (Fig. 3C) influenced the muscle cut-off frequency (Fig. 3D).
204 With a slow twitch (CT-gain: 1.3; light grey lines in Fig. 3C and 3D) the cut-off frequency was 4.3 Hz. The
205 muscle cut-off frequency increased to 4.7 Hz (CT-gain: 1; dark grey lines in Fig. 3C and 3D) and 5.1 Hz
206 (CT-gain: 0.7; black lines in Fig. 3C and 3D) when changing the CT-gain. This implied, as expected, that a
207 fast compound twitch provided the best support for high-frequency force output.

208 The representative power spectra shown in Figure 3B and 3D illustrates that, although there was some
209 overlap in the ranges of the cut-off frequencies for the neural drive and the compound motor unit twitch,
210 these frequencies tended to be higher for the compound motor unit twitch. These tendencies are confirmed
211 when analyzing all simulations, where the compound motor unit twitch cut-off frequency was on average
212 0.54 ± 0.33 Hz higher than the cut-off frequency for the neural drive. This suggests that the neural drive (in
213 particular the recruitment interval) in most conditions is the main determinant of the ability of a muscle to
214 generate rapid force or, alternatively, that the speed of muscle contraction can be boosted by a more rapid
215 drive. The effect of a rapid drive is further enhanced when the motor unit twitches are fast (i.e. when the
216 average motor unit twitch cut-off frequency is high), since in this case the filtering effect of the twitch on the
217 neural drive is minimal and there is a greater margin for an increase in rapidity of the neural drive to impact
218 force speed.

219 Figure 4 shows the ballistic force in two representative simulation conditions. In the first condition (Fig. 4A,
220 4C, 4E), the muscle had a normal range of twitch contraction speeds across the motor units (CT gain = 1) but
221 a fast motor neuron pool (i.e. high initial discharge rate and short recruitment interval). With these settings,
222 RFD was 1,045 %MVC/s. In the second condition (Fig. 4B, 4D, 4F), the muscle had a faster twitch
223 contraction speeds (CT gain = 0.7) but a slower motor neuron pool (i.e., low initial discharge rate and high
224 recruitment interval). With these settings the simulated RFD was reduced by approximately 50% in the
225 second compared to the first condition. This suggests that increasing the motor unit twitch contraction speed
226 by 30% was far from sufficient to compensate for the impact of the slower behavior of the motor neuron
227 pool. This tendency is confirmed when considering all simulation settings (Fig. 5 and 6). In Figure 5, RFD is
228 shown as a function of the recruitment interval for each assigned value for the initial discharge rate (lines in
229 each panel) and for each CT gain (Fig. 5A, 5B, and 5C, respectively). In the simulations shown in Figure 5,
230 the chance of doublets was set to 0%. Overall, RFD was most strongly related to the recruitment interval.
231 Specifically, increasing the recruitment interval from the longest to the shortest simulated value (234 ms to
232 22 ms) implied, on average, an increase in RFD of $1,050 \pm 281$ %MVC/s. This increase was 252 ± 59 %

233 expressed as a relative change. In comparison, an increase in initial discharge rate from lowest to highest rate
234 (89 pps to 212 pps) implied an average increase in RFD of 250 ± 136 %MVC/s, equivalent to 36 ± 13 %,
235 while decreasing the CT-gain (thereby increasing the contraction times) from 1.3 to 0.7 implied an average
236 increase in RFD of 158 ± 149 %MVC/s, equivalent to 20 ± 11 %. The strength of the relation between
237 recruitment interval and RFD was affected by the twitch contraction times, as predicted from the spectral
238 analysis of the neural drive and the compound motor unit twitch (Fig. 3). Specifically, in simulations with a
239 fast muscle (CT-gain=0.7), the difference in average RFD between the shortest and longest recruitment
240 interval (1,641 %MVC/s) was larger than with a slow muscle (CT-gain=1.3; 1,163 %MVC/s).

241 Considering the simulations in which the chance of doublets were varied (Fig. 6) the recruitment range
242 remained the main determinant of RFD. Increase this chance from 0% to 50% implied an average increase in
243 RFD of 205 ± 67 %MVC/s, equivalent to 29 ± 5 %. As indicated in Figure 3, the increase in RFD caused by
244 a higher chance of doublets was largely equivalent to increasing the discharge rate by an equivalent number
245 of action potentials per second.

246

247 DISCUSSION

248 In this study, we systematically investigated the impact of rate coding, recruitment, and contractile properties
249 of a motor unit pool on the maximal RFD during ballistic isometric contractions to a stable near-maximal
250 contraction level. Although all three parameters affected RFD, the rate by which motor units were recruited
251 had the highest impact within the range of simulated values. This observation was confirmed by the spectral
252 analysis of the neural drive and the average muscle twitch force, which showed that the main limiting factor
253 for high-frequency content of the force was indeed motor unit recruitment interval (Fig. 3). Specifically, this
254 implies that the largest improvement in RFD can be achieved by minimizing the recruitment interval within
255 the range of experimentally observed values (Fig. 1).

256 The simulation approach applied in this study cannot reveal whether adaptations in the recruitment interval
257 actually occur in natural conditions. The results, however, suggest that the experimentally observed
258 improvement in RFD following prolonged training of up to 48% (Gruber et al., 2007) likely involved some
259 reduction in the time to full motor unit recruitment, since neither realistic adaptations in twitch contraction
260 time nor changes in rate coding (by means of initial discharge rates or chance of doublets) generated changes
261 in RFD of that magnitude in the simulations (Fig. 5, 6). Indeed, we recently showed indirectly that the
262 increase in RFD in chronically strength/power trained athletes seem to be dependent on a decrease in motor
263 unit recruitment interval before the onset of force (Del Vecchio et al., 2018). Furthermore, it is likely that an
264 increase in initial discharge rate and a higher recruitment rate both can be achieved by an increased
265 magnitude of excitatory synaptic input to the motor neuron pool. Accordingly, a linear relation between the

266 maximal discharge rate of motor neurons and the rate at which motor units are recruited has been shown (Del
267 Vecchio et al., 2019b). In this way, the experimentally observed increase in initial discharge rate after
268 training (Van Cutsem et al., 1998) was likely accompanied by faster motor unit recruitment. It is also
269 possible, although it cannot be fully proved from the results shown, that higher initial discharge rates
270 occurred as an epiphenomenon of neural adaptations aiming to increase RFD by reducing the recruitment
271 interval. The recruitment interval, however, is difficult to estimate experimentally, since in principle it
272 requires complete decomposition of the motor neuron pool, which is not possible with current methods
273 (McGill et al., 2005; Negro et al., 2016). This is underlined by the experimental data adopted for this study,
274 where an average of 12 motor units was decomposed per contraction. Although this is a relatively high
275 number compared to many previous single motor unit studies, it likely represents less than 10% of the motor
276 unit pool (Xiong et al., 2008). Accordingly, the results indicated that the experimentally observed
277 recruitment intervals (Fig. 1B) to some degree underestimated the real interval, since the simulated RFD at,
278 e.g., the average experimentally observed recruitment interval (60 ms; Fig. 1B) were higher ($>800\%$ MVC/s;
279 Fig. 5) than those observed experimentally ($<650\%$ MVC/s; Fig. 1C). To some degree, this uncertainty
280 implies that it is unclear if the full range of simulated values for the recruitment interval (22-232 ms)
281 realistically reflects natural variations across subjects. This uncertainty and the fact that the relative
282 difference between the lowest and highest value of this range of recruitment interval values was higher than
283 for the other parameters implies that the outcome may to some degree overestimate the relative importance
284 of this parameter. However, since variations in recruitment interval had on average >4 times stronger impact
285 on RFD compared to the other parameters, the duration of the recruitment interval would remain the main
286 determinant of RFD even if the natural range for this parameter is somewhat smaller than simulated. For
287 example, if the range of simulated values for the recruitment interval was reduced by 50% (range: 83-173
288 ms), the average relative change in RFD ($65 \pm 11\%$) would still be substantially higher than for the other
289 parameters (Fig. 5).

290 Several previous studies have discussed the neural and muscular determinants of RFD (Duchateau and
291 Baudry, 2014; Folland et al., 2014; Del Vecchio et al., 2019a, 2019b). Duchateau & Baudry argued that the
292 maximal RFD is constrained mainly by the initial motor unit discharge rate, in part based on simulations
293 using a similar model as in this study (Duchateau and Baudry, 2014). Although our results indicate some
294 influence of initial discharge rate and chance of doublets on RFD, it was not identified as the primary
295 determinant. In their simulations, however, only the force generated by four action potentials per motor unit
296 were considered (Duchateau and Baudry, 2014). Since discharge rates are expected to decline rapidly after
297 the first action potentials (Sawczuk et al., 1995; Miles et al., 2005), it is likely that the interval from the onset
298 of the contraction until maximal RFD contain more than four discharges per motor unit. For example, in the
299 simulation illustrated in Fig. 4D and 4F, motor unit #1 exhibited 12 action potentials before maximum RFD
300 was achieved. This implies that considering such low numbers of action potentials (i.e., selecting only those

301 action potentials with low inter-spike interval) may lead to an overestimation of the impact of discharge rate
302 with respect to natural conditions. Furthermore, these previous simulations focused on RFD for single motor
303 unit force and therefore did not reflect the impact of the gradual recruitment of motor units over a certain
304 time interval. Another factor that serves to decrease the impact of initial discharge and chance of doublets on
305 RFD is the non-linear twitch gain illustrated in Fig. 2. These relations imply that for the fastest motor units, a
306 decrease in the discharge rate below 100 pps increases twitch force amplitude, which will to some degree
307 counteract the decrease in twitch summation at lower rates. Finally, Duchateau & Baudry also argued against
308 an impact of changes in contractile properties on RFD. The data underlying this argument, however, was
309 based on the spike-triggered averaging technique (Van Cutsem et al., 1998), which has recently been shown
310 to be highly inaccurate (Dideriksen and Negro, 2018). In another study, Folland and colleagues found that
311 the relative importance of neural and muscular properties changed throughout the time course of the ballistic
312 contraction using an experimental approach (Folland et al., 2014). Here, the neural properties were estimated
313 by the amplitude of the surface electromyographic signal (EMG). The EMG signal, however, cannot
314 differentiate between rate coding and recruitment, which implies that although the study demonstrated that
315 both muscular and neural properties affect maximal RFD, it did not allow for a direct quantification of the
316 impact of properties such as discharge rate, recruitment rate and twitch contraction time. Finally, Del
317 Vecchio and colleagues found that recruitment interval as well as maximal discharge rate predicted maximal
318 RFD (Del Vecchio et al., 2019a, 2019b). To summarize, our study confirms the findings of these previous
319 studies, but extends them by quantifying the relation between each of the three parameters and RFD allowing
320 direct identification of the main determinant for maximal RFD.

321 The simulation approach used in this study has limitations that should be acknowledged. First, the amplitude
322 of the simulated motor unit twitches was not varied across simulations although this has been observed
323 following prolonged resistance training (Van Cutsem et al., 1998; Pääsuke et al., 1999). Adaptations in the
324 twitch amplitude may reflect muscle hypertrophy (Charette et al., 1991; Seynnes et al., 2007) and/or a more
325 efficient transfer of muscle force to the bones (and thus the force transducer) via stiffer tendons (Kubo et al.,
326 2001; Bojsen-Møller et al., 2005; Waugh et al., 2013). Such adaptations increase the effective force
327 producing capacity of the muscle and thereby also RFD when expressed in absolute units (N/s). However,
328 when considering normalized forces as in the current study, a change in the absolute force producing
329 capacity across simulations would not affect the results. A second limitation is that the same discharge rate
330 profiles (uniform initial discharge rate, same rate of discharge rate decline) were assigned to all motor units.
331 In sustained contractions, the peak discharge rate depends on motor unit recruitment threshold (Fuglevand et
332 al., 1993; Barry et al., 2007), but this dependency has not been observed during brief ballistic contractions
333 (Del Vecchio et al., 2019b). It cannot, however, be ruled out that the behavior of the decomposed motor units
334 underlying this study (Fig. 1) may not be representative for the entire motor unit pool, since decomposition
335 based on surface EMG may be more sensitive to superficial units, which have a higher composition of type II

336 units in the tibialis anterior (Henriksson-Larsén et al., 1983). Regarding the decline in discharge rate, it is
337 believed to reflect mainly intrinsic motor neuron properties (Sawczuk et al., 1995; Miles et al., 2005).
338 Nevertheless, it is possible that the synaptic input to motor neurons recruited at the late phase of the ballistic
339 contraction (unlike those recruited from the onset of the contraction) is affected by feedback from muscle
340 afferents (e.g. muscle spindles or Golgi tendon organs) due to the electromechanical delay and nerve
341 conduction times. However, even if systematic variations in discharge rates across the motor unit pool would
342 occur, it will likely have a relatively small effect on RFD (Fig. 5). A third limitation is that the model
343 reflected only one muscle, whereas the force produced by natural joints reflects the activity from synergistic
344 agonist muscles as well as antagonist muscles. However, it has been shown that antagonist muscle activity
345 has little effect on RFD in practice (Folland et al., 2014). Finally, it should be noted that the findings of the
346 study are based on a computational model which reflects a simplified representation of the current
347 understanding of neuromechanical behavior. Consequently, if future experiments invalidate any of the
348 assumption underlying the model, the conclusions of this study should be reconsidered accordingly.
349 Nevertheless, the simulation results are in agreement with previous experimental findings (Del Vecchio et
350 al., 2018), as discussed above.

351 In conclusion, we used a simulation approach to identify the determinants of the ability of muscles to
352 generate rapid force. Although motor unit discharge rates and contractile properties to some degree affected
353 simulated RFD, the interval between recruitment of the first and the last motor unit had the largest impact on
354 this rate. This suggests that the variation in the rate by which motor units are recruited during ballistic
355 contractions across individuals is the main determinant for maximal RFD.

356

357 REFERENCES

- 358 **Barry BK, Pascoe MA, Jesunathadas M, Enoka RM.** Rate coding is compressed but variability is
359 unaltered for motor units in a hand muscle of old adults. *J Neurophysiol* 97: 3206–3218, 2007.
- 360 **Bojsen-Møller J, Magnusson SP, Rasmussen LR, Kjaer M, Aagaard P.** Muscle performance during
361 maximal isometric and dynamic contractions is influenced by the stiffness of the tendinous structures. *J Appl*
362 *Physiol* 99: 986–994, 2005.
- 363 **Burke RE, Rudomin P, Zajac FE.** The effect of activation history on tension production by individual
364 muscle units. *Brain Res* 109: 515–529, 1976.
- 365 **Charette SL, McEvoy L, Pyka G, Snow-Harter C, Guido D, Wiswell RA, Marcus R.** Muscle
366 hypertrophy response to resistance training in older women. *J Appl Physiol* 70: 1912–1916, 1991.

- 367 **Christie A, Kamen G.** Doublet Discharges in Motoneurons of Young and Older Adults. *J Neurophysiol* 95:
368 2787–2795, 2006.
- 369 **Van Cutsem M, Duchateau J, Hainaut K.** Changes in single motor unit behaviour contribute to the
370 increase in contraction speed after dynamic training in humans. *J Physiol* 513 (Pt 1: 295–305, 1998.
- 371 **Desmedt JE, Godaux E.** Ballistic contractions in man: characteristic recruitment pattern of single motor
372 units of the tibialis anterior muscle. *J Physiol* 264: 673–693, 1977a.
- 373 **Desmedt JE, Godaux E.** Fast motor units are not preferentially activated in rapid voluntary contractions in
374 man. *Nature* 267: 717–719, 1977b.
- 375 **Desmedt JE, Godaux E.** Ballistic contractions in fast or slow human muscles; discharge patterns of single
376 motor units. *J Physiol* 285: 185–196, 1978.
- 377 **Dideriksen JL, Negro F.** Spike-triggered averaging provides inaccurate estimates of motor unit twitch
378 properties under optimal conditions. *J Electromyogr Kinesiol* 43: 104–110, 2018.
- 379 **Duchateau J, Baudry S.** Maximal discharge rate of motor units determine the maximal rate of force
380 development during ballistic contractions in human. *Front Hum Neurosci* 8, 2014.
- 381 **Enoka RM, Fuglevand AJ.** Motor unit physiology: some unresolved issues. *Muscle Nerve* 24: 4–17, 2001.
- 382 **Folland JP, Buckthorpe MW, Hannah R.** Human capacity for explosive force production: Neural and
383 contractile determinants. *Scand J Med Sci Sport* 24: 894–906, 2014.
- 384 **Fuglevand AJ, Winter DA, Patla AE.** Models of recruitment and rate coding organization in motor-unit
385 pools. *J Neurophysiol* 70: 2470–2488, 1993.
- 386 **Granit R, Kernell D, Shortess GK.** Quantitative aspects of repetitive firing of mammalian motoneurons,
387 caused by injected currents. *J Physiol* 168: 911–931, 1963.
- 388 **Gruber M, Gruber SBH, Taube W, Schubert M, Beck SC, Gollhofer A.** Differential effects of ballistic
389 versus sensorimotor training on rate of force development and neural activation in humans. *J Strength Cond*
390 *Res* 21: 274–282, 2007.
- 391 **Henriksson-Larsén KB, Lexell J, Sjöström M.** Distribution of different fibre types in human skeletal
392 muscles. I. Method for the preparation and analysis of cross-sections of whole tibialis anterior. *Histochem J*
393 15: 167–178, 1983.
- 394 **Jenkins NDM, Housh TJ, Buckner SL, Bergstrom HC, Smith CM, Cochrane KC, Hill EC, Miramonti**

- 395 **AA, Schmidt RJ, Johnson GO, Cramer JT.** Four weeks of high- versus low-load resistance training to
396 failure on the rate of torque development, electromechanical delay, and contractile twitch properties. *J*
397 *Musculoskelet Neuronal Interact* 16: 135–144, 2016.
- 398 **Kubo K, Kanehisa H, Fukunaga T.** Effects of different duration isometric contractions on tendon elasticity
399 in human quadriceps muscles. *J Physiol* 536: 649–655, 2001.
- 400 **Kudina LP, Andreeva RE.** Repetitive doublet firing of motor units: Evidence for plateau potentials in
401 human motoneurons? *Exp Brain Res* 204: 79–90, 2010.
- 402 **Matthews PB.** Relationship of firing intervals of human motor units to the trajectory of post-spike after-
403 hyperpolarization and synaptic noise. *J Physiol* 492: 597–628, 1996.
- 404 **McGill KC, Lateva ZC, Marateb HR.** EMGLAB: An interactive EMG decomposition program. *J Neurosci*
405 *Methods* 149: 121–133, 2005.
- 406 **Miles GB, Dai Y, Brownstone RM.** Mechanisms underlying the early phase of spike frequency adaptation
407 in mouse spinal motoneurons. *J Physiol* 566: 519–532, 2005.
- 408 **Moritz CT, Barry BK, Pascoe MA, Enoka RM.** Discharge rate variability influences the variation in force
409 fluctuations across the working range of a hand muscle. *J Neurophysiol* 93: 2449–2459, 2005.
- 410 **Mrówczyński W, Celichowski J, Raikova R, Krutki P.** Physiological consequences of doublet discharges
411 on motoneuronal firing and motor unit force. *Front Cell Neurosci* 9, 2015.
- 412 **Negro F, Muceli S, Castronovo AM, Holobar A, Farina D.** Multi-channel intramuscular and surface EMG
413 decomposition by convolutive blind source separation. *J Neural Eng* 13, 2016.
- 414 **Pääsuke M, Ereline J, Gapeyeva H.** Twitch contractile properties of planter flexor muscles in power and
415 endurance trained athletes. *Eur J Appl Physiol Occup Physiol* 80: 448–451, 1999.
- 416 **de Ruyter CJ, Kooistra RD, Paalman MI, de Haan A.** Initial phase of maximal voluntary and electrically
417 stimulated knee extension torque development at different knee angles. *J Appl Physiol* 97: 1693–1701, 2004.
- 418 **Sawczuk A, Powers RK, Binder MD.** Spike frequency adaptation studied in hypoglossal motoneurons of
419 the rat. *J Neurophysiol* 73: 1799–1810, 1995.
- 420 **Schmidtbleicher D, Haralambie G.** Changes in contractile properties of muscle after strength training in
421 man. *Eur J Appl Physiol Occup Physiol* 46: 221–228, 1981.
- 422 **Seynnes OR, de Boer M, Narici M V.** Early skeletal muscle hypertrophy and architectural changes in

423 response to high-intensity resistance training. *J Appl Physiol* 102: 368–373, 2007.

424 **Del Vecchio A, Falla D, Felici F, Farina D.** The relative strength of common synaptic input to motor
425 neurons is not a determinant of the maximal rate of force development in humans. *J Appl Physiol* 127: 205–
426 214, 2019a.

427 **Del Vecchio A, Negro F, Falla D, Bazzucchi I, Farina D, Felici F.** Higher muscle fiber conduction
428 velocity and early rate of torque development in chronically strength trained individuals. *J Appl Physiol* 125:
429 1218–1226, 2018.

430 **Del Vecchio A, Negro F, Holobar A, Casolo A, Folland JP, Felici F, Farina D.** You are as fast as your
431 motor neurons: speed of recruitment and maximal discharge of motor neurons determine the maximal rate of
432 force development in humans. *J. Physiol.* (2019b). doi: 10.1113/JP277396.

433 **Waugh CM, Korff T, Fath F, Blazeovich AJ.** Rapid force production in children and adults: Mechanical
434 and neural contributions. *Med Sci Sports Exerc* 45: 762–771, 2013.

435 **Xiong GX, Zhang JW, Hong Y, Guan Y, Guan H.** Motor unit number estimation of the tibialis anterior
436 muscle in spinal cord injury. *Spinal Cord* 46: 696–702, 2008.

437

438 FIGURE CAPTIONS

439 Figure 1: Distribution of experimentally observed values for initial discharge rate (A), recruitment interval
440 (B), and time to reach 80% MVC (C) across 20 subjects. This data was adopted from (Del Vecchio et al.,
441 2019b).

442 Figure 2: The non-linear gain of the 2nd (black line), 3rd (dark grey line) and 4th-nth twitch during summation
443 of overlapping twitches as a function of the inter-spike interval (ISI) normalized to the contraction time (CT).
444 Symbols indicate the experimental data reported by Burke et al. 1976. The two additional x-axes indicate the
445 relation between the twitch gains and the non-normalized discharge rate for a slow-twitch motor unit
446 (contraction time: 90 ms) and a fast-twitch motor unit (contraction time: 30 ms).

447 Figure 3: Time (A) and frequency (B) domain representations of the neural drive in four different simulation
448 conditions with different initial discharge rates (IDR), recruitment intervals (RI) and/or chance of doublets
449 (DC) . The neural drives depicted in A were the smoothed cumulative spike trains (40 ms hamming
450 window). In this way, the rate indicated on the y-axis represents the rate of action potentials across the motor
451 unit pool. The power spectra of the neural drive were derived from the interval from the onset of the
452 contraction until the simulated force reached the point of maximal RFD. For all four simulations in panels A

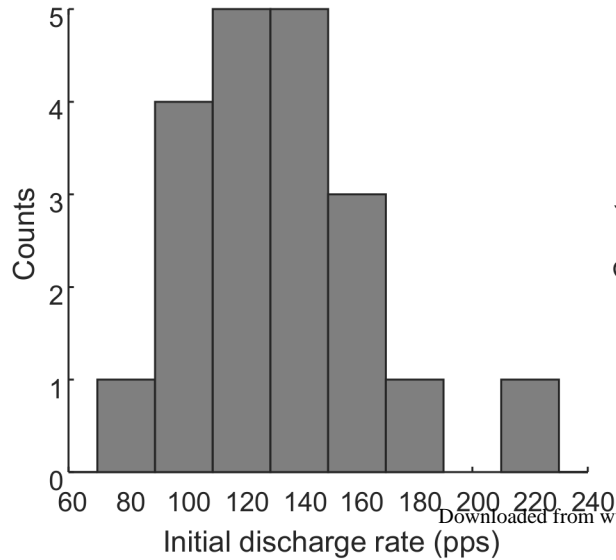
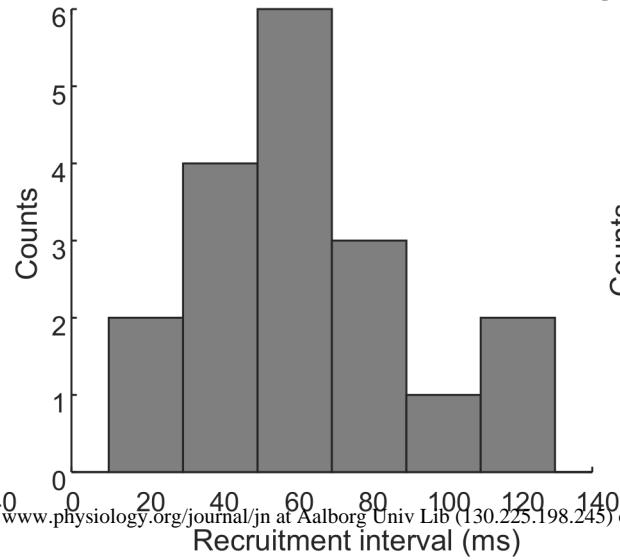
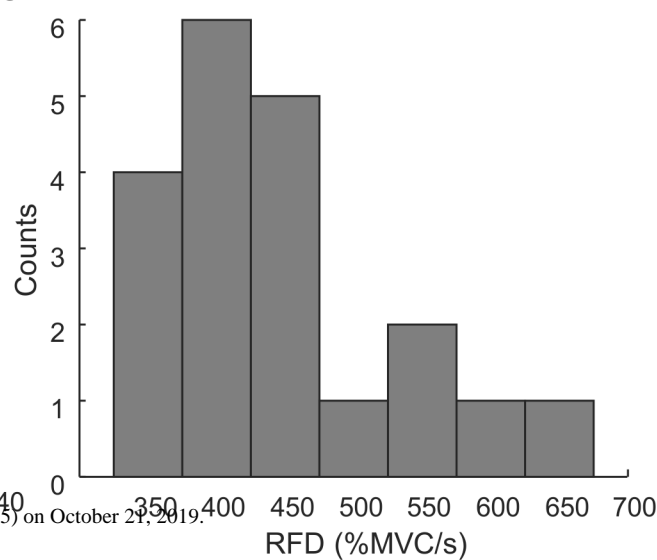
453 and B the CT gain was 1. In B, the circles indicate the cut-off frequency. Time (C) and frequency (D)
454 domain representations of the cumulative motor unit twitch during three different simulation conditions: CT
455 gain = 1.3 (slow muscle); CT gain = 1 (normal muscle); CT gain = 0.7 (fast muscle). The power spectra of
456 the cumulative motor unit twitches were derived from the interval equivalent to the time it took for the
457 simulated force to reach the point of maximal RFD. For all three simulations the initial discharge rate was
458 132 pps, the recruitment interval was 82 ms and the chance of doublets was 0%. In D, the circles indicate the
459 cut-off frequency.

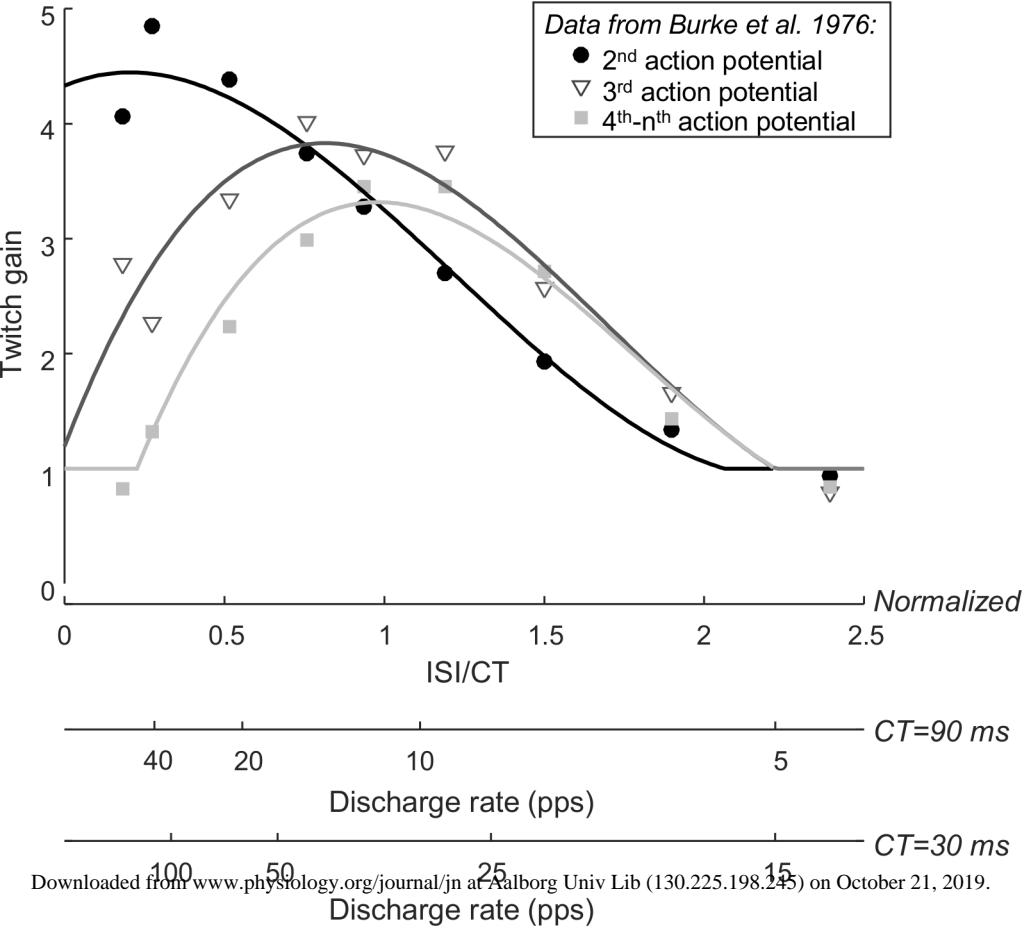
460 Figure 4: Two representative simulations illustrating the effects of the muscular and neural model parameters
461 on the rate of force development. Panels A and B show the distribution of contraction times across the motor
462 unit pool. Panels C and D show the motor unit discharge patterns for the smallest (#1) and largest (#188)
463 motor unit. Here, each symbol indicates the instantaneous discharge rate of one motor unit during the first
464 250 ms of the contraction. Panels E and F show the simulated forces. The left column represents a model
465 with a normal muscle (motor unit contraction times between 30 and 90 ms) and a fast motor neuron pool
466 (relatively high initial discharge rate (IDR) and short recruitment interval), while the right column represents
467 the opposite: a model with a fast muscle and a relatively slow motor unit pool. In both simulations, the
468 chance of doublets was set to 0%.

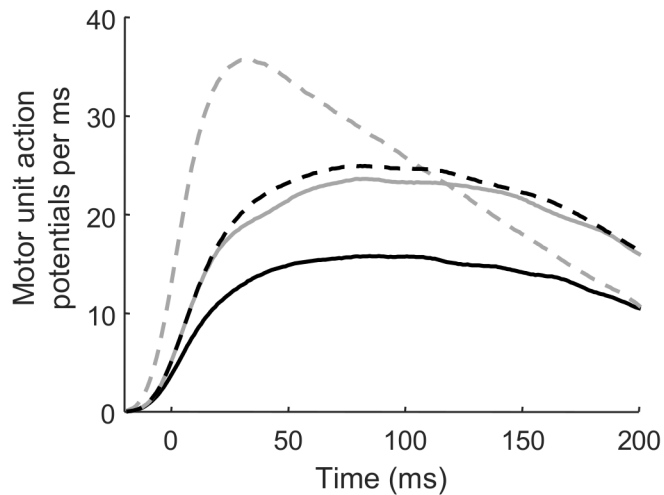
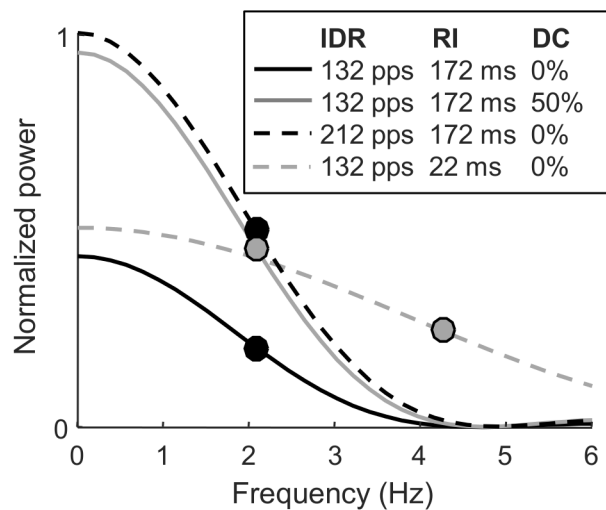
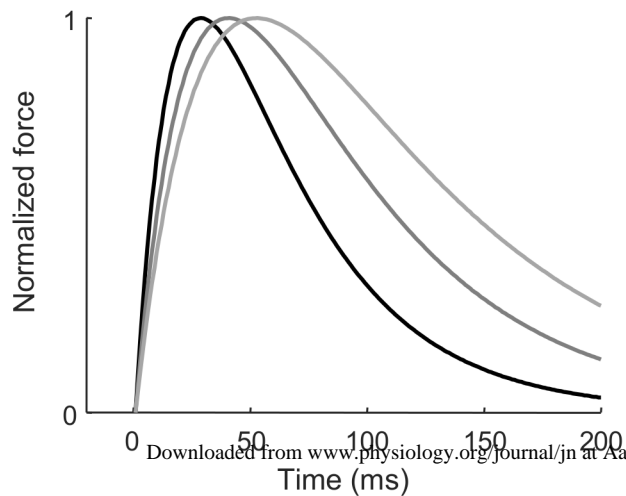
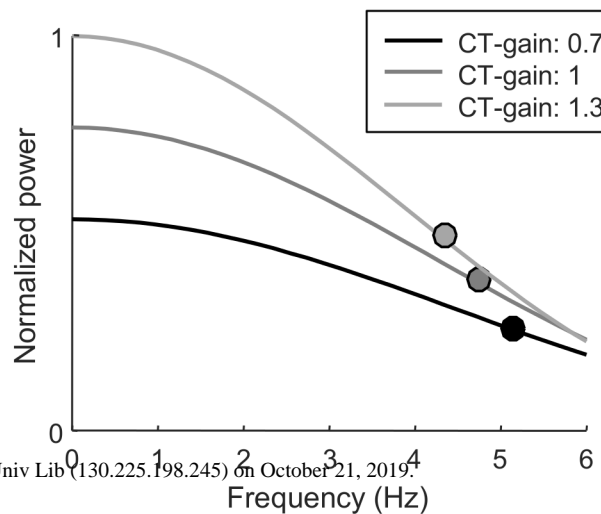
469 Figure 5: Average RFD as a function of recruitment interval for all initial discharge rates and for all
470 contraction time gains in simulations with 0% chance of doublets. Panel A represents contraction time gain
471 of 0.7 (fastest muscle), panel B represents contraction time gain of 1 (normal muscle), and panel C represents
472 contraction time gain of 1.3 (slow muscle). The lines in each panel represent simulations with different initial
473 motor unit discharge rates.

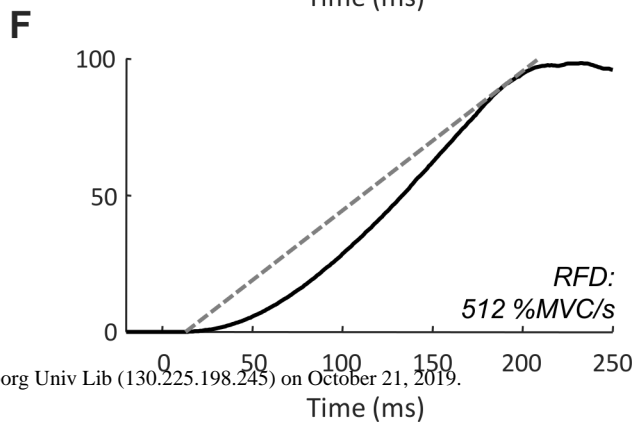
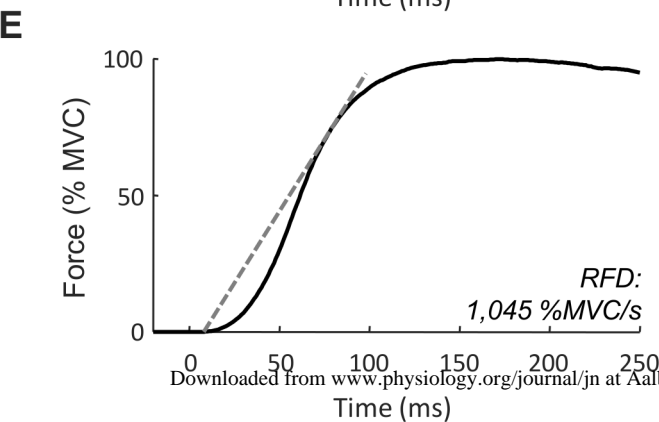
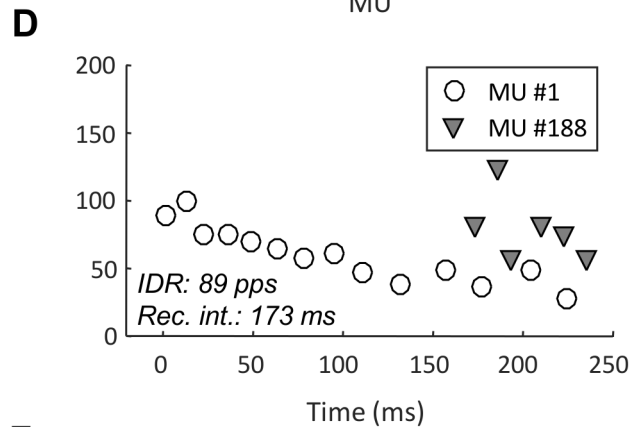
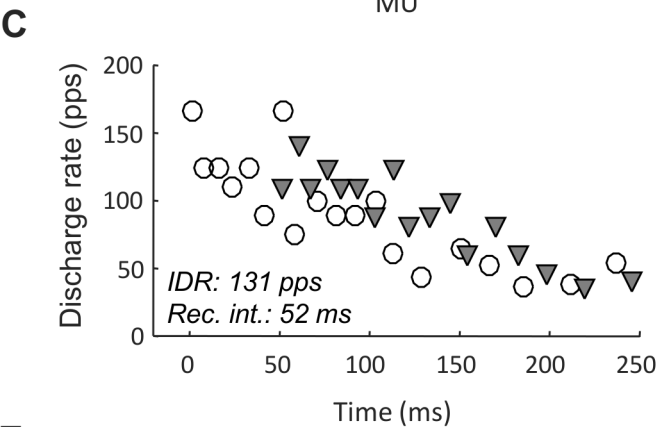
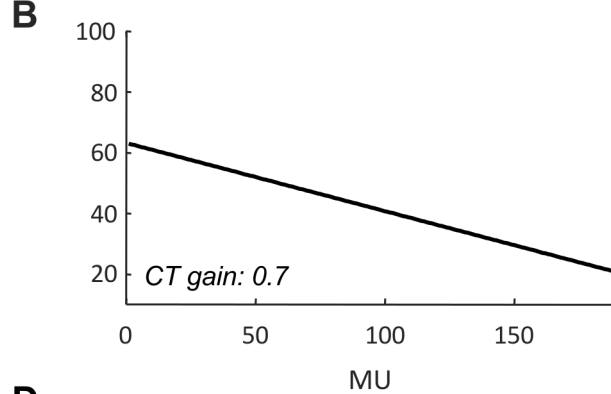
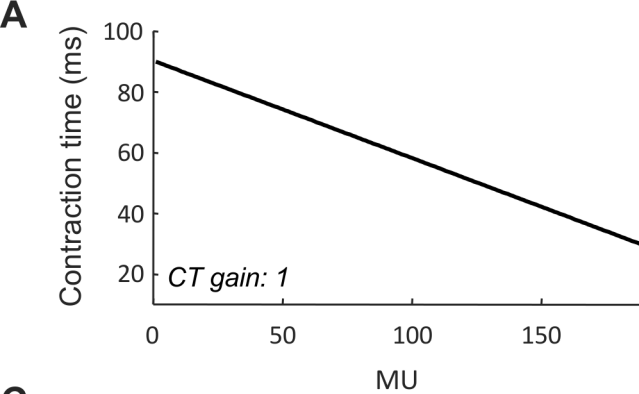
474 Figure 6: Average RFD as a function of recruitment interval for across all percentages assigned to the change
475 of doublets occurring and for all contraction time gains in simulations with initial discharge rates of 132 pps.
476 Panel A represents contraction time gain of 0.7 (fastest muscle), panel B represents contraction time gain of
477 1 (normal muscle), and panel C represents contraction time gain of 1.3 (slow muscle). The lines in each
478 panel represent simulations with different chances of doublets.

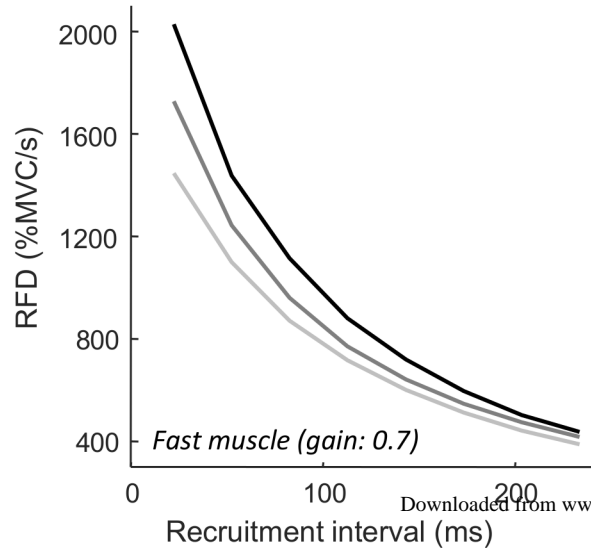
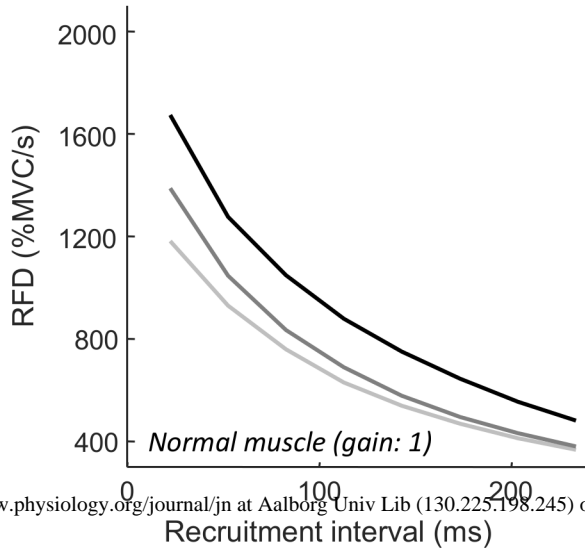
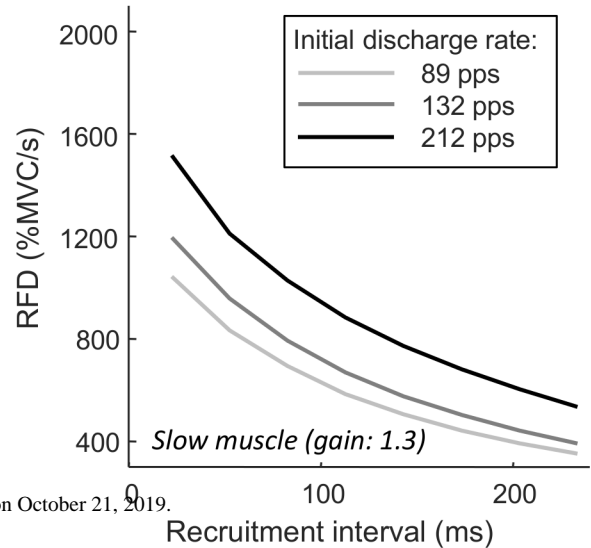
479

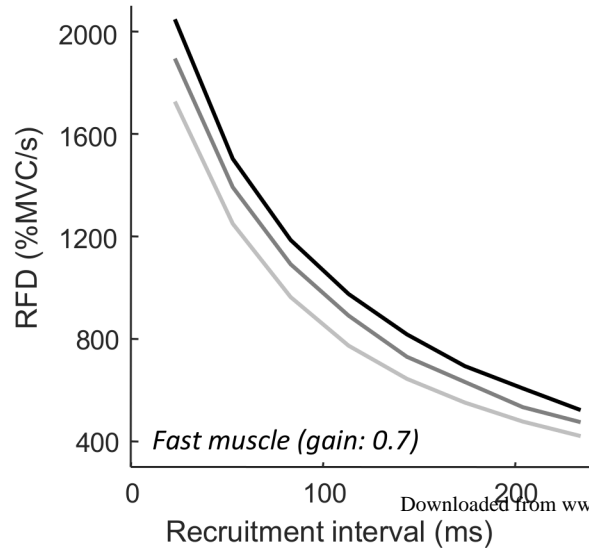
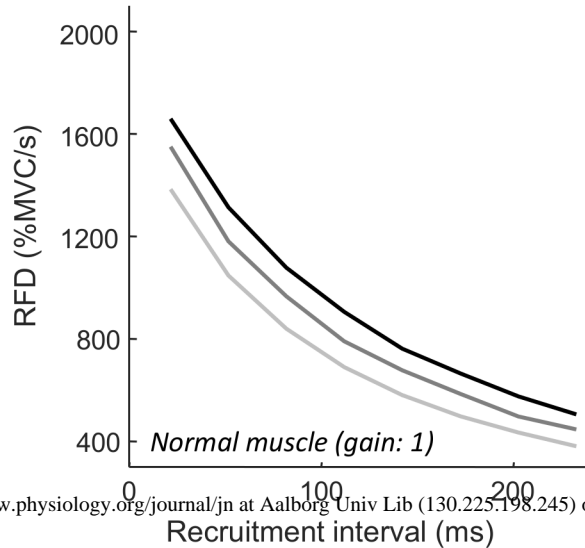
A**B****C**



A**B****C****D**



A**B****C**

A**B****C**